

See discussions, stats, and author profiles for this publication at: <https://www.researchgate.net/publication/335893421>

Performance analysis of inertial twist morphing concept in hovering flight

Conference Paper · September 2019

CITATIONS

0

READS

85

5 authors, including:



[Mohammadreza Amoozgar](#)
University of Hddersfield

30 PUBLICATIONS 89 CITATIONS

[SEE PROFILE](#)



[Alexander David Shaw](#)
Swansea University

51 PUBLICATIONS 374 CITATIONS

[SEE PROFILE](#)



[Jiaying Zhang](#)
Swansea University

26 PUBLICATIONS 60 CITATIONS

[SEE PROFILE](#)



[Chen Wang](#)
Nanjing University of Aeronautics & Astronautics

18 PUBLICATIONS 48 CITATIONS

[SEE PROFILE](#)

Some of the authors of this publication are also working on these related projects:



Semi Aeroelastic Hinge - AlbatrossOne [View project](#)



Structural Design of composite structures [View project](#)

PERFORMANCE ANALYSIS OF INERTIAL TWIST MORPHING CONCEPT IN HOVERING FLIGHT

M.R. Amoozgar, A.D. Shaw, J. Zhang, C. Wang, M.I. Friswell

College of Engineering, Swansea University, Swansea, Wales SA2 8PP, United Kingdom

Abstract

This paper presents the initial performance analysis of a twist morphing concept based on moving a mass in the chordwise direction in hovering flight. The blade structure is considered to be made of composite materials with bend-twist coupling present in the layup. The chordwise movement of the added mass introduces an additional lag moment along the spar of the blade which is able to change the twist of the blade through the bend-twist coupling. Therefore, the twist of the blade is related to the mass position in the chordwise direction and its magnitude. The blade is modelled by using the geometrically exact fully intrinsic beam equations, and the aerodynamic loads are simulated by using the quasi-steady aerodynamic model combined with uniform inflow. The governing aeroelastic equations are discretized using a time-space scheme. The results show that when the mass moves in the chordwise direction of the blade, the twist distribution of the blade changes. This twist change results in variation of the aerodynamic loads and hence change the aerodynamic performance of the rotor. The results highlighting the importance of the added mass location and magnitude, and the lag-twist coupling value on the reduction in the rotor power required is presented.

1. INTRODUCTION

The helicopter has many advantages such as vertical takeoff and landing, and hovering which makes it unique. Currently, the helicopter blade shape is designed through a compromise between various flight conditions, and therefore the final shape is not optimal all flight cases. This results in higher levels of noise, pollution, fuel consumption, and lower levels of performance and comfort. Therefore, the idea of changing the shape of the blade, either locally or globally, has been proposed. The adaptive helicopter is a means of implementing morphing technologies to design helicopter blades to enhance the performance, or to reduce the noise and vibration of the rotorcraft. Among all possible concepts for morphing a blade, the twist and trailing edge flap concepts have received the most attention over the past two decades [1]. Several different ideas for the control of a blade, including twist, pitch, flap, and camber, were reviewed by Straub and Chopra, and the advantages and disadvantages of these methods for vibration reduction were reported [2, 3]. The change in the blade twist during flight is the focus of this paper. When a rotorcraft is in the hover condition, highly twisted blades are optimal, while low levels of twist are optimal for high-speed forward velocities [4]. Therefore, the predefined blade twist variation is normally chosen as a compromise between different flight conditions. Blade twist morphing changes the blade twist actively during flight to allow the rotorcraft to fly in an optimum condition

in terms of twist variation. Han et al. [5] showed how the performance of a helicopter during flight could be improved by dynamic blade twist. They demonstrated that the dynamic blade twist improves the performance and reduces the rotor power requirement.

One of the earliest studies concerning the twist change of the blade via piezoelectric actuators was performed by Chen and Chopra [6]. In this study, the piezoelectric patches were located on the lower and upper surfaces of the blade, and about 0.4° of twist change was achieved at 4 per rev. This concept was tested in the hover and it was found that a linear twist change of about 0.6° may result in a 10% increase in the rotor lift [7]. Chattopadhyay et al. [8] used smart materials to reduce and control the vibratory load of a composite box beam blade. They showed that the number of actuators and their location significantly affects the blade dynamic load reduction. The dynamic behaviour of active twist rotor blades with distributed anisotropic strain actuators for vibration and noise reduction has been investigated experimentally and analytically by Cesnik et al. [9]. Good correlation between their developed analytical model and the experimental results was reported. This study was continued to check the developed analytical model for the forward flight condition by Shin and Cesnik [10]. Thakkar and Ganguli [11] considered the vibration reduction of a soft in plane hingeless rotor blade in forward flight with induced shear based on piezoceramic actuation. They showed that about

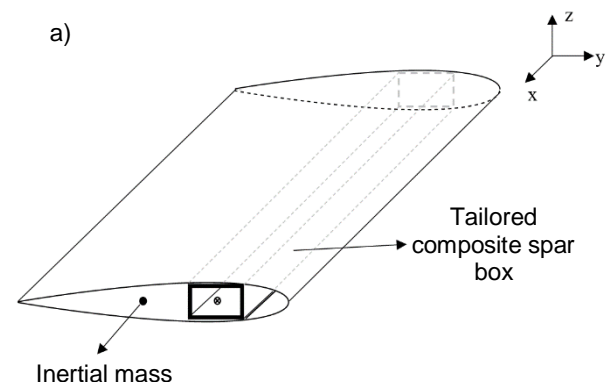
43% reduction in the vibration is feasible. Schultz [12] proposed a new concept capable of large shape morphing with a small energy input based on bi-stable structures. The active vibration reduction of composite hingeless rotor blades with dissimilarity based on the active twist concept was investigated by Prashant and Sung [13]. The numerical results showed that the blade dissimilarities influence the rotor vibratory loads and the input energy. You et al. [14] examined the influence of different actuation scenarios to maximize the performance of a rotor in high-speed flight conditions. Apart from using piezo materials for blade morphing, there are some other efforts focusing on using shape memory alloys for blade twist change. Prahlad and Chopra [15] presented the concept of using a shape memory alloy torque tube to change the twist distribution of a tiltrotor blade between hover and forward flight. The effect of heat treatment of the SMAs in tuning the actuation behaviour was discussed. The development and experiment of an active twist rotor blade using a thermo-mechanical shape memory alloy was reported by Bushnell et al. [16]. In the ONR-funded Reconfigurable Rotor Blade program the SMA actuator was used to change the twist of a V-22 Osprey blade [17-19]. It was shown that about 2° of twist change is feasible with this SMA concept [18]. Pagano et al. [20] proposed an SMA rod mechanism for morphing helicopter blades to mitigate the environmental impact. There are also other concepts in the literature for changing the twist of the blades. One concept for twist variation of the blade is the warp-induced twist which originally was proposed for fixed-wing applications [21], and then extended to rotary-wing aircraft [4]. In this concept, the ribs can rotate freely around the spar, and the skin is also free to move on the ribs. The warping is generated by creating a relative motion in the span-wise direction by using a threaded rod, and when this rod rotates the result is a twist change of the blade.

More recently, several promising concepts have been proposed through the Shape Adaptive Blades for Rotorcraft Efficiency (SABRE) project. Within SABRE, six different morphing concepts have been proposed all aiming to enhance the performance, or to reduce the vibration or energy requirements of the rotor system. The final vision of SABRE is to use multiple morphing concepts in a single blade to achieve potentially greater benefits than possible through just one morphing technology. One of the concepts that has been considered is to change of the twist of the blade in flight by moving a mass in the chordwise direction as discussed by Amoozgar et al. [22-25]. In this concept the change of the blade twist is obtained by moving a mass near the tip of the blade to

create a local centrifugal force which then, through the lag-twist coupling of the composite layup, results in a torsional moment. This torsional moment is then able to change the twist of the blade. In this paper, the proposed concept is first introduced, and the important parameters are summarized. Then an analytical model capable of examining this concept is developed, and the effect of different system parameters and their influence on the twist of the blade and also the performance of the rotor are presented.

2. PROBLEM STATEMENT

As shown in Figure 1, a composite hingeless rotor blade is considered. The blade is modelled by a cantilever beam which is rotating at a constant rotational velocity. The blade is assumed to have a composite cross-section so that it has some specific sort of elastic couplings. A mass is added to the blade, near to the tip of the blade, to generate an additional centrifugal force. The mass can be moved in the chordwise direction, y , by using a proper mechanism. When the mass is moved, a variable lag moment is produced about the spar of the blade. This lag bending moment turns into an equivalent torsional moment through the lag-twist coupling available in the composite layup. Therefore, the blade twist can be changed by moving the mass in the chordwise direction of the blade. The mass location in the x and y directions are denoted here by x_m and y_m , and it is assumed that the mass is located centrally in the thickness direction. The blade length and chord are denoted by L and c , respectively, and the blade rotates at a constant speed Ω_0 . When the mass is moved, the twist of the blade changes, which in turn the performance of the rotor can be altered. Therefore, in this study, the effect of this proposed twist morphing concept on the performance of the rotor is investigated.



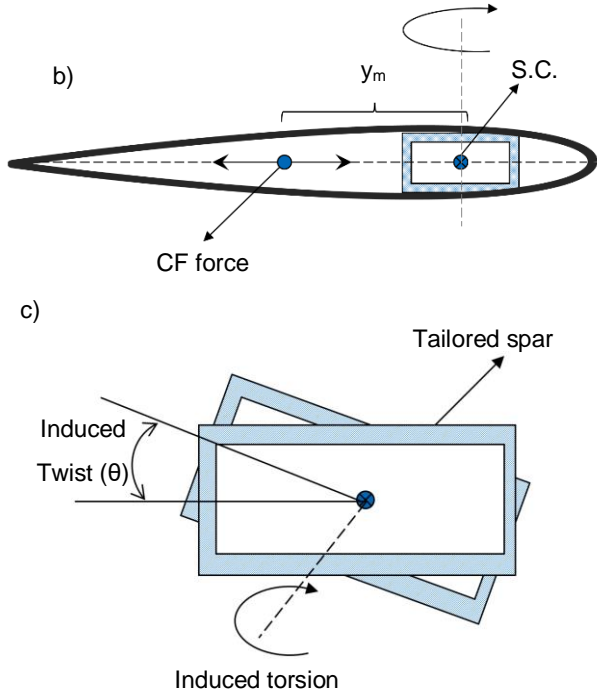


Figure 1: Schematic description of the twist morphing concept a) spanwise position of the mass b) chordwise position of the mass c) twisted section

3. FORMULATION

In this section, the aeroelastic formulation of the composite blade is introduced. The composite blade structure is modelled by using the geometrically exact fully intrinsic beam equations as follows

$$\begin{aligned}
 & \partial F_1 / \partial x_1 + K_2 F_3 - K_3 F_2 = \partial P_1 / \partial t + \Omega_2 P_3 - \Omega_3 P_2 \\
 & \partial F_2 / \partial x_1 + K_3 F_1 - K_1 F_3 = \partial P_2 / \partial t + \Omega_3 P_1 - \Omega_1 P_3 \\
 & \partial F_3 / \partial x_1 + K_1 F_2 - K_2 F_1 = \partial P_3 / \partial t + \Omega_1 P_2 - \Omega_2 P_1 \\
 & \partial M_1 / \partial x_1 + K_2 M_3 - K_3 M_2 + 2\gamma_{12} F_3 - 2\gamma_{13} F_2 = \\
 & \partial H_1 / \partial t + \Omega_2 H_3 - \Omega_3 H_2 + V_2 P_3 - V_3 P_2 \\
 & \partial M_2 / \partial x_1 + K_3 M_1 - K_1 M_3 + 2\gamma_{13} F_1 - (1 + \gamma_{11}) F_3 = \\
 & \partial H_2 / \partial t + \Omega_3 H_1 - \Omega_1 H_3 + V_3 P_1 - V_1 P_3 \\
 (1) \quad & \partial M_3 / \partial x_1 + K_1 M_2 - K_2 M_1 + (1 + \gamma_{11}) F_2 - 2\gamma_{12} F_1 = \\
 & \partial H_3 / \partial t + \Omega_1 H_2 - \Omega_2 H_1 + V_1 P_2 - V_2 P_1 \\
 & \partial V_1 / \partial x_1 + K_2 V_3 - K_3 V_2 + 2\gamma_{12} \Omega_3 - 2\gamma_{13} \Omega_2 = \\
 & \partial \gamma_{11} / \partial t \\
 & \partial V_2 / \partial x_1 + K_3 V_1 - K_1 V_3 - (1 + \gamma_{11}) \Omega_3 + 2\gamma_{13} \Omega_1 = \\
 & 2\partial \gamma_{12} / \partial t \\
 & \partial V_3 / \partial x_1 + K_1 V_2 - K_2 V_1 + (1 + \gamma_{11}) \Omega_2 - 2\gamma_{12} \Omega_1 = \\
 & 2\partial \gamma_{13} / \partial t \\
 & \partial \Omega_1 / \partial x_1 + K_2 \Omega_3 - K_3 \Omega_2 = \partial \kappa_1 / \partial t \\
 & \partial \Omega_2 / \partial x_1 + K_3 \Omega_1 - K_1 \Omega_3 = \partial \kappa_2 / \partial t \\
 & \partial \Omega_3 / \partial x_1 + K_1 \Omega_2 - K_2 \Omega_1 = \partial \kappa_3 / \partial t
 \end{aligned}$$

where F_i and M_i for $i=1, \dots, 3$, are the internal forces and moments in the three directions, and V_i and Ω_i are the components of linear and angular velocities. P_i and H_i define the linear and angular momenta. The generalized strain components are denoted by γ_{1i} and κ_i , and K_i gives the final values of twist and curvatures of the beam as follows

$$(2) \quad K_i = \kappa_i + k_i$$

where the initial curvature and twist of the blade in the undeformed coordinate is defined by k_i for $i=1, \dots, 3$.

It is noted that, to derive the intrinsic equations of the beam, the three-dimensional strain energy is solved for the warping, and the asymptotically correct one-dimensional variables are obtained through a rigorous dimensional reduction [26].

The cross-sectional stiffness matrix, which defines the relationship between the internal forces and moments to the generalized strains, is defined as

$$(3) \quad \begin{bmatrix} F_1 \\ F_2 \\ F_3 \\ M_1 \\ M_2 \\ M_3 \end{bmatrix} = \begin{bmatrix} S_{11} & S_{12} & S_{13} & S_{14} & S_{15} & S_{16} \\ S_{12} & S_{22} & S_{23} & S_{24} & S_{25} & S_{26} \\ S_{13} & S_{23} & S_{33} & S_{34} & S_{35} & S_{36} \\ S_{14} & S_{24} & S_{34} & S_{44} & S_{45} & S_{46} \\ S_{15} & S_{25} & S_{35} & S_{45} & S_{55} & S_{56} \\ S_{16} & S_{26} & S_{36} & S_{46} & S_{56} & S_{66} \end{bmatrix} \begin{bmatrix} \gamma_{11} \\ 2\gamma_{12} \\ 2\gamma_{13} \\ \kappa_1 \\ \kappa_2 \\ \kappa_3 \end{bmatrix}$$

In this study, it is assumed that only the diagonal elements of this matrix and the S_{46} term (i.e. the lag-twist coupling) are non-zero. This is not generally true for a general composite structure and the matrix is generally full. However, in this study the focus is on the lag-twist coupling, and hence this assumption is reasonable.

In the next step, the aerodynamic loads applied on the blade in hover condition is introduced. For this study, the aerodynamic loads are simulated by using the intrinsic expression of Greenberg's theory [27] is defined as

$$\begin{aligned}
 & \mathbf{f}_{aero} = \mathbf{C}^{Ba} \mathbf{f}_a \\
 (4) \quad & \mathbf{m}_{aero} = \mathbf{C}^{Ba} \mathbf{m}_a + \mathbf{C}^{Ba} \mathbf{x}_a \mathbf{f}_a
 \end{aligned}$$

where \mathbf{x}_a is the offset between the beam reference line and the aerodynamic centre, and \mathbf{C}^{Ba} is the direction cosine matrix of deformed frame with respect to aerodynamic frame. In this study, it is assumed that the offset of the aerodynamic centre from the elastic axis is zero. The aerodynamic force and moment equations in the aerodynamic reference frame are [27]

$$f_a = \rho_\infty b \begin{bmatrix} 0 \\ c_{l_a} V_{a3}^2 - c_{d_0} V_T V_{a2}^2 + c_{d_a} V_{a3} V_{a2} \\ -c_{l_a} V_{a2} \left(V_{a3} - \frac{\Omega_a b}{2} \right) - \frac{c_{l_a} \dot{V}_{a3} b}{2} - c_{d_0} V_T V_{a3} + c_{d_a} V_{a3}^2 \end{bmatrix} \quad (5)$$

$$m_a = 2\rho_\infty b^2 \begin{bmatrix} -b c_{l_a} V_{a2} \Omega_a / 8 - c_{l_a} (b^2 \dot{\Omega}_a / 32 - b \dot{V}_{a3} / 8) \\ 0 \\ 0 \end{bmatrix}$$

where c_{l_a} , c_{d_0} , and c_{d_a} are the airfoil lift and drag coefficients, respectively. The variables with subscript ($_a$) are expressed in the aerodynamic reference frame. The induced inflow velocity corrects the vertical component of the velocity as follows

$$V_{a3T} = V_{a3} + \lambda \quad (6)$$

The uniform induced inflow velocity determined by the blade element momentum theory at $\frac{3}{4}$ span, λ , is given as [28]

$$\lambda = \operatorname{sgn}[\theta + \phi(0.75R)] \frac{\pi\sigma}{8} \Omega R \times \left(\sqrt{1 + \frac{12}{\pi\sigma} |\theta + \phi(0.75R)|} - 1 \right) \quad (7)$$

where σ is the blade solidity, and θ and ϕ are the blade pitch angle and elastic twist angle, respectively.

By combining the structural formulation with the aerodynamic model, the full aeroelastic model is obtained. To solve the nonlinear aeroelastic equations, a time-space discretization scheme is used [26]. In this method, every unknown variable is defined on the right and left hand sides of each node. This is appropriate to take into account any discontinuity such as the point mass. Finally, the equations of motion are summarized in a compact form as

$$a_{ji} \dot{q}_i + b_{ji} q_i + c_{jik} q_i q_k = 0 \quad (8)$$

where q is the vector containing the unknown parameters (F_i , M_i , V_i , Ω_i , $i=1..3$) at the left and right side of each node, and a_{ji} , b_{ji} , c_{jik} are the matrices of linear and nonlinear coefficients. The steady state condition of the system is determined by removing all time derivative terms and solving the resultant nonlinear equations by the Newton-Raphson method.

Finally, to close the composite blade formulations, the following boundary conditions are considered:

$$F_{1,2,3}(R, t) = 0, M_{1,2,3}(R, t) = 0, \\ V_{1,2,3}(0, t) = 0, \Omega_{1,2}(0, t) = 0, \Omega_3(0, t) = \Omega_0$$

4. RESULTS

A hingeless rotor blade that resembles the main rotor blade of the BO-105 with the characteristics reported in Table 1 is considered ([29]).

Table 1: Parameters of the BO-105 main rotor blade

Item	Value
Radius (m)	4.91
Chord (m)	0.27
Pre-cone angle (deg)	2.5°
Rotating velocity (rad/s)	44.4

It is noted that the BO-105 blade has variable spanwise properties, but here it is assumed that the equivalent blade has uniform spanwise properties. The cross-sectional properties of the equivalent uniform blade are selected so that the fundamental frequencies of the blade are as close as possible to the BO-105 blade.

Table 2: Comparison of the equivalent blade frequencies with those of the BO-105 blade

Mode	Present (Hz)	Peterson et al. [29] (HZ)
1 st Lag	4.61	4.66
1 st Flap	7.52	7.91
2 nd Flap	20.03	19.64
1 st Torsion	25.40	26.78
2 nd Lag	29.8	30.6

To achieve these frequencies, a GA optimization algorithm was used, and the proper cross-sectional properties are obtained. The comparison between the fundamental frequencies of the equivalent blade and the BO-105 blade are reported in Table 2. From here on, all the results are based on the equivalent blade.

As mentioned before, the lag-twist coupling plays a significant role in this concept and hence the lag-twist stiffness term, i.e. S_{46} , exists and is related to the torsional stiffness (S_{44}) and bending stiffness (S_{66}) through the following relation:

$$S_{46} = \alpha \cdot \sqrt{S_{44} \cdot S_{66}} \quad (9)$$

where α is the nondimensional bend-twist coupling index which can have a value between $-1 \leq \alpha \leq 1$ [30]. It is assumed here that this term is added to the blade stiffness matrix without altering other properties.

A non-structural mass is added to the blade to produce an extra centrifugal force. The added mass value is considered to be a fraction of the

blade mass itself as follows

$$(10) \quad \eta = m_m / \mu \cdot R$$

First, the effect of moving the added mass on the twist change of the blade is determined. Figure 2 shows the blade tip twist change when the added mass moves from most forward position to the most aft position. In this case, when the leg-twist coupling is $\alpha=0.8$, and the added mass is $\eta=0.1$, about 33° of twist change is achievable at the tip of the blade. However, it must be noted that due to aeroelastic instability problems, it is not possible to freely move the mass toward the trailing edge of the section, and the permitted design space is limited.

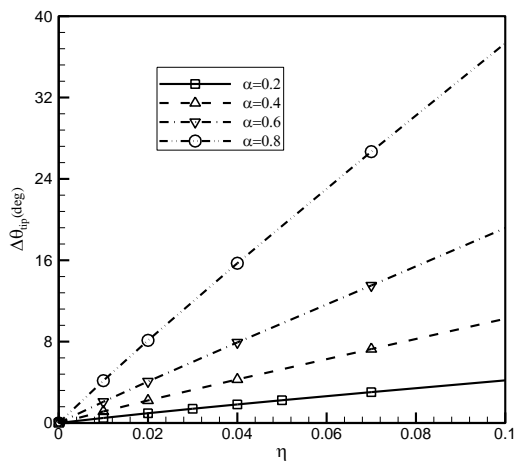


Figure 2: Change of blade tip twist for different coupling and mass ratio values

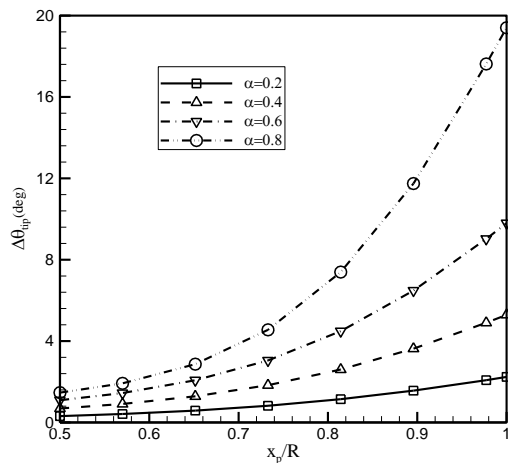


Figure 3: Change of blade tip twist for different coupling values and different spanwise locations

The effect of the spanwise location of the added mass on the tip twist change of the blade is determined next and shown in Figure 3. By

moving the mass toward the tip of the blade, the twist value increases rapidly due to the increase in the centrifugal force. Therefore, in terms of the twist change, it is more advantageous to place the mass near the tip of the blade, although this may not be the best option due to other restrictions.

Next the effect of this concept on the performance of the rotor in hovering flight is determined. First the rotor performance of the equivalent rotor blade is obtained and compared with the experimental results reported in [31] and shown in Figure 4. The results are a good match, and the discrepancy is mostly due to the use of a simple aerodynamic model and also using the equivalent blade with constant properties instead of the actual blade. However, since the main focus of this paper is on the rotor power saving/reduction of the proposed morphing concept, this difference will not affect the results and conclusion. The figure of merit of the rotor with the equivalent blade is obtained and compared with experiments in Figure 5. Again, the results are a good match.

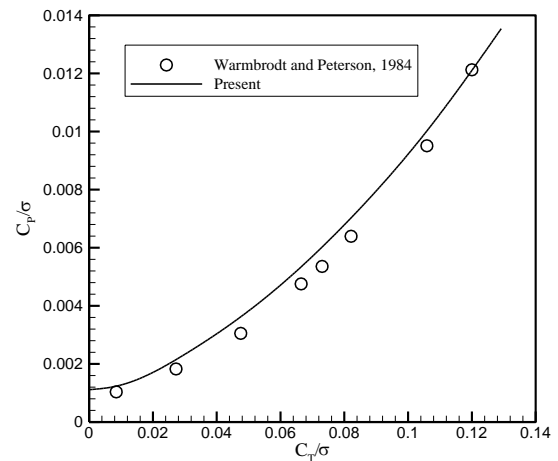


Figure 4: Comparison of the rotor performance to the experimental data from [31]

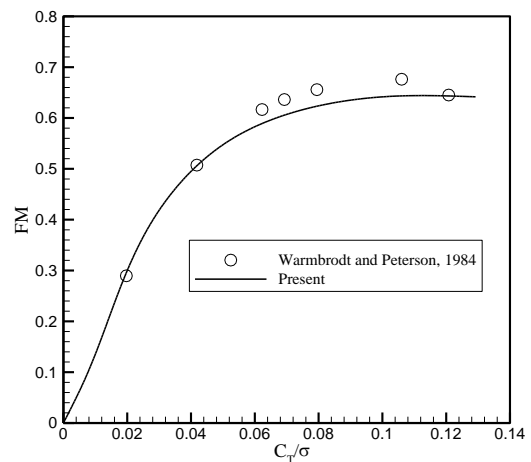


Figure 5: Comparison of the rotor figure of merit to the experimental data from [31]

As mentioned earlier, when the mass is moved in the chordwise direction of the section, the twist of the blade changes. This twist change can result in a reduction in the required power. Figure 6 shows the rotor power reduction for different values of lag-twist coupling. For all values of coupling, the power reduction increases by increasing the thrust ratio. In this case, 5 percent mass ($\eta=0.05$) is added to the blade and the chordwise movement of the mass is $y_m/c=-0.25$. Furthermore, by increasing the coupling value, the power reduction value increases. This is because when the coupling value increases, the twist change increases. It must be noted that if the mass could be moved further toward the trailing edge of the section, more power reduction is achieved. But in this case, above the point $y_m/c < -0.25$, the blade experiences aeroelastic instability. Therefore, in this paper, the mass chordwise movement is limited to this point. However, it is possible to optimise the system by considering the aeroelastic stability constraints to gain more power reduction, but this is beyond the scope of this paper.

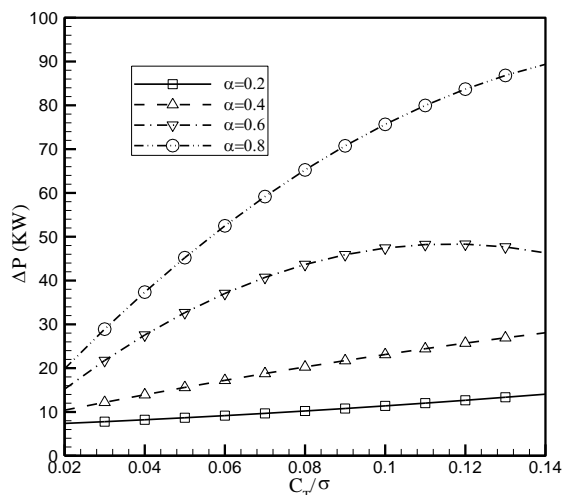


Figure 6: Rotor power reduction for different values of coupling for $y_m/c=-0.25$ and $\eta=0.05$

Figure 7 shows the effect of lag-twist coupling of the composite blade on the change in the rotor figure of merit for different thrust ratios. It is clear that the lag-twist coupling influences the rotor figure of merit. This shows that the change in the figure of merit is completely dependent to the thrust ratio and also the lag-twist coupling value. Note that, in this case, the maximum achievable figure of merit is about $\Delta FM= 0.06$ which is achieved at $CT/\sigma=0.14$ and $\alpha=0.6$.

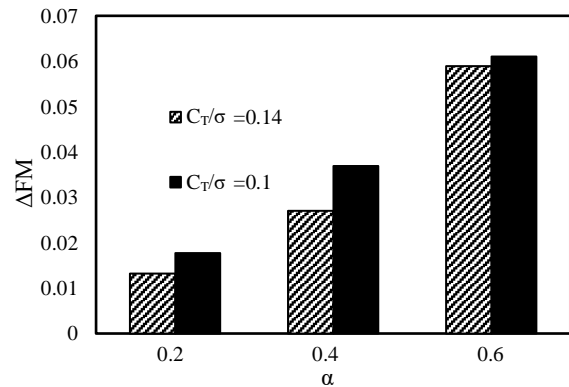


Figure 7: Rotor figure of merit enhancement for different values of coupling and thrust ratios for $y_m/c=-0.25$ and $\eta=0.05$

Next, the effect of the added mass on the rotor power reduction is obtained and shown in Figure 8. In this case, the mass is moved to $y_m/c=-0.25$, and the lag-twist coupling is $\alpha=0.8$. By increasing the added mass, the rotor power requirement reduces. This highlights that the added mass value significantly affects the power requirement of the rotor.

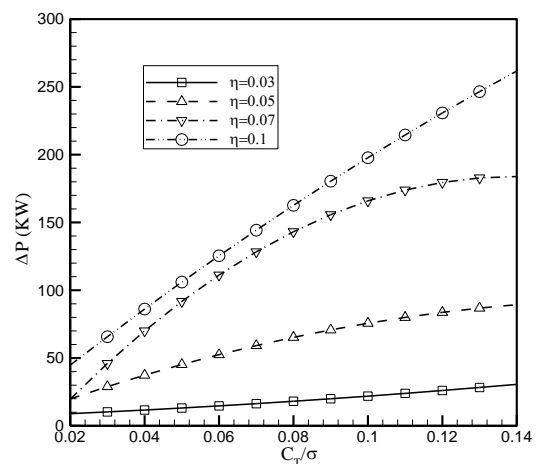


Figure 8: Rotor power reduction for different values of mass ratio for $\alpha=0.8$ and $y_m/c=-0.25$

Finally, the effect of chordwise location of the added mass on the rotor power requirement is calculated and shown in Figure 9. In this case, the mass ratio is $\eta=0.05$, and the lag-twist coupling value is $\alpha=0.8$. This shows that when the mass is moved to the trailing edge of the blade section, more power reduction is achieved. This is because when the mass is moved toward the trailing edge of the blade, the amount of twist change increases.

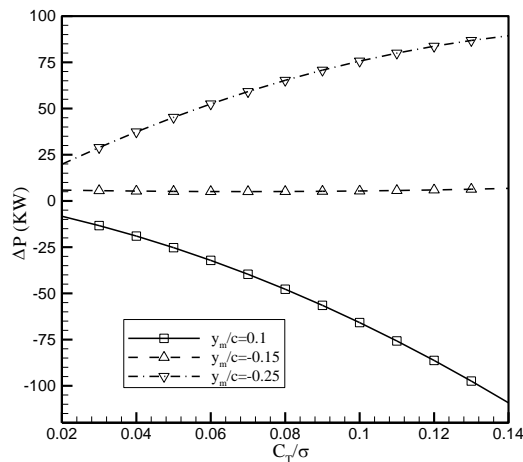


Figure 9: Rotor power reduction for different values of chordwise mass locations for $\alpha=0.8$ and $\eta=0.05$

5. CONCLUSION

In this paper, a new morphing concept capable of changing the twist of the helicopter blade in flight is introduced. The concept is based on a movable mass that can produce an additional centrifugal force. This centrifugal force and its resultant lag moment turn into an equivalent torsional moment through the lag-twist coupling present in the composite layup of the cross-section. The blade structure is modelled by using the fully intrinsic beam equations, and the aerodynamic loads applied of the blade are simulated by using quasi-steady lifting line theory combined with a uniform inflow. The governing aeroelastic equations are discretised using a proper time-space scheme. The results show that the twist distribution of the blade depends on the mass magnitude, mass location, and also the lag-twist coupling of the cross-section. Then required power of the rotor is estimated and it is shown that this morphing concept can result in a reduction in the power required. Finally, it has been shown that the added mass magnitude, location, and also the elastic coupling of the composite cross-section influence the rotor required power and can enhance the figure of merit of the rotor.

Acknowledgements

This research leading to these results has received funding from the European Commission under the European Union's Horizon 2020 Framework Programme 'Shape Adaptive Blades for Rotorcraft Efficiency' grant agreement 723491.

References

1. Maucher, C. K., Grohmann, B. A., and Jäker, P. "Review of adaptive helicopter rotor blade actuation concepts," *Proceedings of the 9th Adaptronic Congress, Göttingen, Germany*, 2005.
2. Friedrich, K. S. "A feasibility study of using smart materials for rotor control," *Smart Materials and Structures* Vol. 5, No. 1, 1996, p. 1.
3. Chopra, I. "Review of State of Art of Smart Structures and Integrated Systems," *AIAA Journal* Vol. 40, No. 11, 2002, pp. 2145-2187.
4. Mistry, M., Gandhi, F., Nagelsmit, M., and Gurdal, Z. "Actuation Requirements of a Warp-Induced Variable Twist Rotor Blade," *Journal of Intelligent Material Systems and Structures* Vol. 22, No. 9, 2011, pp. 919-933.
5. Han, D., Pstrikakis, V., and Barakos, G. N. "Helicopter flight performance improvement by dynamic blade twist," *Aerospace Science and Technology* Vol. 58, 2016, pp. 445-452.
6. Chen, P. C., and Chopra, I. "Induced strain actuation of composite beams and rotor blades with embedded piezoceramic elements," *Smart Materials and Structures* Vol. 5, No. 1, 1996, p. 35.
7. Chen, P. C., and Chopra, I. "Hover Testing of Smart Rotor with Induced-Strain Actuation of Blade Twist," *AIAA Journal* Vol. 35, No. 1, 1997, pp. 6-16.
8. Chattopadhyay, A., Liu, Q., and Gu, H. "Vibration Reduction in Rotor Blades Using Active Composite Box Beam," *AIAA Journal* Vol. 38, No. 7, 2000, pp. 1125-1131.
9. Cesnik, C. E. S., Shin, S., and Wilbur, M. L. "Dynamic response of active twist rotor blades," *Smart Materials and Structures* Vol. 10, No. 1, 2001, p. 62.
10. Shin, S. J., and Cesnik, C. "Forward flight response of the active twist rotor for helicopter vibration reduction," *19th AIAA Applied Aerodynamics Conference*. American Institute of Aeronautics and Astronautics, 2001.
11. Thakkar, D., and Ganguli, R. "Helicopter vibration reduction in forward flight with induced-shear based piezoceramic actuation," *Smart Materials and Structures* Vol. 13, No. 3, 2004, p. 599.
12. Schultz, M. R. "A Concept for Airfoil-like Active Bistable Twisting Structures," *Journal of Intelligent Material Systems and Structures* Vol. 19, No. 2, 2008, pp. 157-169.
13. Pawar, P. M., and Jung, S. N. "Active twist control methodology for vibration reduction of a helicopter with dissimilar rotor system," *Smart Materials and Structures* Vol. 18, No. 3, 2009, p. 035013.

14. You, Y. H., Jung, S. N., and Kim, C. J. "Optimal deployment schedule of an active twist rotor for performance enhancement and vibration reduction in high-speed flights," *Chinese Journal of Aeronautics* Vol. 30, No. 4, 2017, pp. 1427-1440.
15. Prahlad, H., and Chopra, I. "Design of a variable twist tilt-rotor blade using shape memory alloy (SMA) actuators," *SPIE's 8th Annual International Symposium on Smart Structures and Materials*, 2001.
16. Bushnell, G. S., Arbogast, D., and Ruggeri, R. "Shape control of a morphing structure (rotor blade) using a shape memory alloy actuator system," *Proceedings of SPIE Smart Structures and Materials*, 2008.
17. Ruggeri, R. T., Jacot, A. D., and Clingman, D. J. "Shape memory actuator systems and the use of thermoelectric modules," *SPIE's 9th Annual International Symposium on Smart Structures and Materials*. Vol. 4698, SPIE, 2002, p. 9.
18. Ruggeri, R., Arbogast, D., and Bussom, R. "Wind Tunnel Testing of a Lightweight One-Quarter-Scale Actuator Utilizing Shape Memory Alloy," *49th AIAA/ASME/ASCE/AHS/ASC Structures, Structural Dynamics, and Materials Conference, 16th AIAA/ASME/AHS Adaptive Structures Conference, 10th AIAA Non-Deterministic Approaches Conference, 9th AIAA Gossamer Spacecraft Forum, 4th AIAA Multidisciplinary Design Optimization Specialists Conference*. American Institute of Aeronautics and Astronautics, 2008.
19. Clingman, D., and Jacot, D. "Shape Memory Alloy Consortium and demonstration," *41st Structures, Structural Dynamics, and Materials Conference and Exhibit*. American Institute of Aeronautics and Astronautics, 2000.
20. Pagano, A., Ameduri, S., Cokonaj, V., Prachar, A., Zachariadis, Z., and Drikakis, D. "Helicopter blade morphing strategies aimed at mitigating environmental impact," *Journal of Theoretical and Applied Mechanics* Vol. 49, No. 4, 2011, pp. 1233-1259.
21. Vos, R., Gurdal, Z., and Abdalla, M. "Mechanism for Warp-Controlled Twist of a Morphing Wing," *Journal of Aircraft* Vol. 47, No. 2, 2010, pp. 450-457.
22. Amoozgar, M. R., Shaw, A. D., Zhang, J., and Friswell, M. I. "Composite Blade Twist Modification by Using a Moving Mass and Stiffness Tailoring," *AIAA Journal*, 2018, pp. Accepted, DOI: 10.2514/1.J057591.
23. Amoozgar, M. R., Shaw, A. D., Zhang, J., and Friswell, M. I. "Twist morphing of a hingeless rotor blade using a moving mass," *44th European Rotorcraft Forum*. Delft, The Netherlands, 2018.
24. Amoozgar, M. R., Shaw, A. D., Zhang, J., and Friswell, M. I. "The effect of a movable mass on the aeroelastic stability of composite hingeless rotor blades in hover," *Journal of Fluids and Structures* Vol. 87, 2019, pp. 124-136.
25. Amoozgar, M. R., Shaw, A. D., Zhang, J., Wang, C., and Friswell, M. I. "Lag-twist coupling sensitivity and design for a composite blade cross-section with D-spar," *Aerospace Science and Technology* Vol. 91, 2019, pp. 539-547.
26. Hodges, D. H. "Geometrically Exact, Intrinsic Theory for Dynamics of Curved and Twisted Anisotropic Beams," *AIAA Journal* Vol. 41, No. 6, 2003, pp. 1131-1137.
27. Amoozgar, M. R., Shahverdi, H., and Nobari, A. S. "Aeroelastic Stability of Hingeless Rotor Blades in Hover Using Fully Intrinsic Equations," *AIAA Journal* Vol. 55, No. 7, 2017, pp. 2450-2460.
28. Gessow, A., and Mayers, G. C., Jr. *Aerodynamics of the Helicopter*. Fredrick Ungar Publishing Company, New York, New York, 1967.
29. Peterson, R. L., Field, M., Johnson, W., and Alto, P. "Aeroelastic loads and stability investigation of a full-scale hingeless rotor," *NASA Technical Memorandum 103867*, 1991.
30. Ong, C. H., and Tsai, S. W. "Design, manufacturing and testing of a bend-twist D-spar," *Stanford University, SAND 99-1324*, 1999.
31. Warmbrodt, W., and Peterson, R. L. "Hover test of a full-scale hingeless rotor," *NASA Technical Memorandum 85990*, 1984.